Superconducting Nanowire Detectors for the Electron Ion Collider

Date of submission: May 29, 2020
Project Leader: Whitney Armstrong
Contact Person: Whitney Armstrong
eRD #:
Project Members:

Whitney Armstrong, Sylvester Joosten, Jihee Kim, Zein-Eddine Meziani,
Valentine Novosad, Chao Peng, Tomas Polakovic, Junqi Xi

Argonne National Laboratory

Abstract

Superconducting Nanowire Single Photon Detectors (SNSPDs) have become the dominant technology in quantum optics due to their unparalleled timing resolution and quantum efficiency. We are proposing to transform this technology into a particle detector for the EIC. Recently, we have demonstrated detector operation in magnetic fields greater than 5 T at high rate with high efficiency. Leveraging these results and detector timing resolution as low as $\lesssim 20$ ps, this project will produce a small (mm^2) superconducting nanowire pixel array for detecting high energy particles. This first of its kind detector will have the flexibility to be used in multiple far forward detector systems, and will extend the scientific reach of the EIC.

Contents

1 Introduction

Superconducting nanowire single photon detectors (SNSPD) have, since their initial discovery [1], found many applications in fields of nanophotonics and quantum communication. Metrics like sub-20 ps timing jitter [2], nearly 100% quantum efficiency up to IR wavelength [3, 4] and count rates as high as 10^9 counts/s with effectively zero dark counts [5] make them the go-to choice in many applications, including LIDAR systems [6], quantum teleportation [7], quantum key distribution [8], optical quantum computing [9], and many others [10]. Many, if not all, of these applications leverage the unique capability of detecting individual photons with unprecedented timing resolution and low noise.

We propose to develop superconducting nanowire detectors for applications at the Electron Ion Collider. The targeted R&D will focus on developing a novel particle tracking detector for environments requiring radiation-hard pixel sensors to operate in high magnetic fields at cryogenic temperatures at high rates while providing excellent position and timing resolution.

In section 2, we motivate the detector R&D with a discussion of some high-impact science enabled by this new detector technology. Next, in section 3, the design, construction, and theory of operation for SNSPDs is presented. From a discussion of photon detection, we then shift to a brief review of their use as *particle* detectors, and conclude with a discussion of possible detector concepts for the EIC. Section 4 outlines the proposed plan for developing and testing an array of superconducting nanowire sensors, along with articulating the R&D milestones and deliverables for the project. Finally, the requested budget is presented in section 5 along with a narrative for the various funding scenarios.

2 Motivation

Looking to the future Electron Ion Collider [11], there will exist numerous opportunities to leverage the capabilities of superconducting nanowire detectors and enhance the scientific program. It worth noting that currently the EIC User's Group is engaged in a community-wide effort to write a so-called Yellow Report for the EIC [12, 13], and many of the detector requirements are still being worked out by the Physics Working Group [14]. Here we emphasize the physics of the far forward hadron region where high energy hadrons, with very little transverse momentum, need to be detected. In this region, challenges arise when instrumenting very close to the ion beam, especially as the beam position and size vary as each fill of ions is accelerated. Radiation damage, high magnetic fields, and cryogenic temperatures put constraints on location and space for detectors in this region where hermetic detection is ideal.

2.1 Motivating EIC Science

Some of the big questions motivating the construction of an EIC were highlighted in a recent assessment from the National Academies of Sciences, Engineering, and Medicine [15]. These questions are:

- How does the mass of the nucleon arise?
- How does the spin of the nucleon arise?
- What are the emergent properties of dense systems of gluons?

The world's first polarized electron and polarized ion collider aims to address these questions. Furthermore, a large number of deep exclusive and semi-inclusive processes will be measured at the EIC, forming the hadron tomography experimental program which aims to produce 3D images (or distributions) of polarized quarks and gluons in nucleons and nuclei. The far forward detector requirements for the science outlined in the white paper [11] is nicely presented in a previously approved proposal to develop Roman Pot detectors [16]. Here we build on this motivation and discuss some important physics not fully articulated or directly addressed in the white paper.

2.1.1 Origin of the Proton Mass

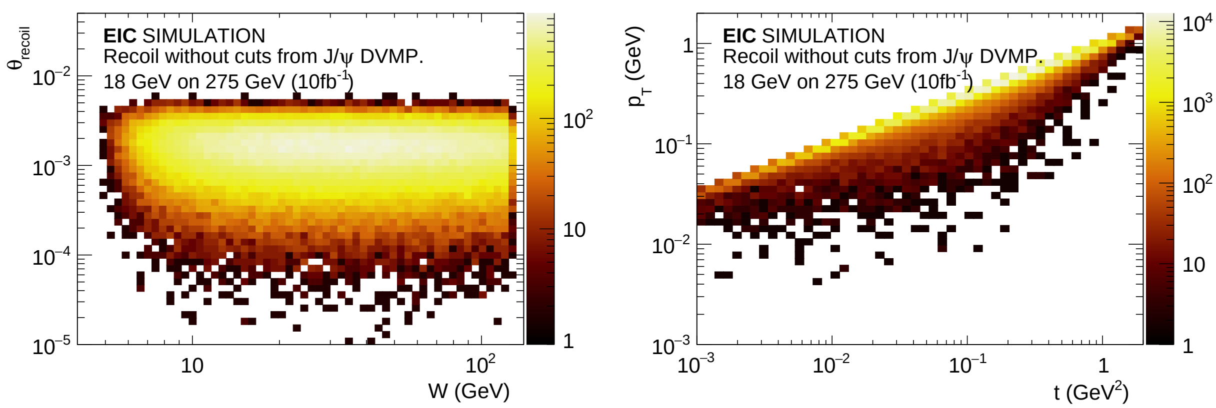

Figure 1: Recoil kinematics for J/ψ production at a high-energy EIC configuration. The left panel shows the recoil angle (in radians) as a function of W, while the right panel shows the recoil p_T as a function of the Mandelstam variable t.

Protons and neutrons are responsible for 99% of the mass of the visible universe. Modern calculations indicate that the proton mass is dynamical in origin and almost entirely unaffected by the value of the quark mass. The origin of the nucleon's mass is a hot topic in nuclear science, highlighted in the 2015 Long Range Plan for Nuclear Science : "*The vast majority [...] is due to* *quantum fluctuations of quark-antiquark pairs, the gluons and the energy associated with quarks moving around close to the speed of light*". Furthermore, the 2018 NAS report for the EIC identified the origin of the nucleon mass as one of the most important profound questions to be addressed at an EIC.

The proton mass is intimately related to the trace anomaly of the QCD energy-momentum tensor, experimentally accessible through the quarkonium (J/ψ and Υ) photo-production cross section near threshold. Alternatively, the trace anomaly can also be accessed through the interference between J/ψ photo-production and Bethe-Heitler pair production near the J/ψ threshold.

Far-forward recoil acceptance will be critical to maximize the potential program of this fundamental program at the EIC. Figure 1 shows the recoil kinematics at a higher-energy EIC configuration. The recoil proton is restricted to very small angles. Small angle/low p_T acceptance will be particularly important to measure the differential production cross sections for events with $t \sim t_{\text{min}}$.

2.1.2 Tomography of Nuclei

The nuclear tomography program at the EIC will reveal the 3-dimensional quark and gluon structure of nuclear matter. Unraveling this information involves measuring multiple fully exclusive hard scattering processes to extract the generalized parton distributions (GPDs) [17]. The quark and gluon GPDs encode a position space tomographic image of hadronic matter, and measuring these processes is a significant part of the scientific program at Jefferson Lab and for the future EIC.

The most prominent exclusive process involving GPDs is deeply virtual Compton scattering (DVCS). At EIC kinematics, the reaction $p(e, e'\gamma p)$ requires measuring a forward scattered proton in addition to the scattered electron and electro-produced photon. In the case of DVCS on the proton, the typical momentum transfers cause the proton to scatter at intermediate to small angles, which will be detected by a forward detector or far forward detector.

But the nuclear tomography program is not limited to just the proton! Light (and not so light) nuclei are of significant interest too. For example, coherent DVCS on ^{4}He has been recently measured [18] and is the subject of a group of upcoming experiments at JLab [19]. However, for collider kinematics at fixed momentum transfer, as the as mass of the nucleus increases the scattered angle becomes smaller. Measuring these ions at very small angles is quite difficult and is often done in a Roman pot type configuration 10s of meters downstream of the interaction point. Because of the extremely small angle, and small momentum transfer relative to the ion beam energy, the recoiling ion looks a lot like the unperturbed ion beam.

2.1.3 Other Processes

Other processes requiring far forward detection were identified in a recent Physics Working Group summary talk [14]. Charged current e-p cross-sections and asymmetries will need detection pushed as far forward as possible to extract important quantities like the polarized sea quark distributions and the high-x $\bar{s}$ distribution. Also, the Jets and Heavy Flavor physics working subgroup identified very forward detection and displaced vertex resolutions to be important for the open heavy flavor measurements.

3 Superconducting Nanowire Sensors

3.1 Photon Detectors

A superconducting nanowire detector is a microelectronic device that utilizes critical phenomena in superconductivity to transform energy or heat into electrical signal. Typical realization of a nanowire detector pixel can be seen in Figure 2: The sensitive area (usually on the order of $20 \times 20\ \mu\mathrm{m}^2$) is covered by a densely packed superconducting nanostrip with a cross-section of roughly 10×100 nm^2 and a total length of approximately 1 mm. The narrow detecting wire is connected to wider superconducting leads that can connect it to other pixels or contact pads for a 2-wire electronic readout which also doubles as the current supply. The sensitive area of the device can be increased by connecting multiple pixels in parallel, increasing detection rate proportional to number of sub-pixels and decreasing signal by a factor inversely proportional to this number. As typical signals are usually on the order of $10\,\mathrm{mV}$, this is not a fundamental concern.

Nanowire photon detector operation The detection process of a SNSPD can be divided into stages which are roughly sketched in Figure 3. First, a very thin and narrow nanowire is maintained well below the superconducting critical temperature T_C and is constant-current biased at current values close to critical currents (Figure 3a). Absorption of a single photon with energy much higher than the superconducting energy gap $\hbar\omega \gg 2\Delta \approx 2\ \mathrm{meV}$ will lead to excitation of two quasi-electrons with high kinetic energies, and those will begin to inelastically scatter with other quasi-particles in the system. This forms the initial so-called hotspot [20] (Figure 3b). The approximate time-scales associated with this process are on the order of 10 ps [21] (dictated by the electron-phonon scattering times). The next stage of the detection process is the expansion of the hotspot (Figure 3c). First, the quasi-particles further multiply due to inelastic scattering and move diffusively outwards, towards the edges of the nanowire. The depletion of Cooper pairs leads to local reduction of the order parameter and redistribution of the current in the region [22]. If the nanowire is biased close to critical currents, the current density in the hotspot region rises above the critical values and the superconducting state vanishes completely creating a normal state region that bisects the superconducting wire (Figure 3d). As the section of the wire turns normal, a voltage drop is generated across the wire and this voltage spike is registered as a resistance spike which corresponds to a single photon detection event. In the last stage, the current bias is reduced, either passively through a parallel resistive shunt, or actively using electronically controlled current source and the hot spot shrinks and vanishes, preparing the nanowire for the next detection event (Figure 3e).

Through this process, a single particle, which would conventionally cause a signal well below

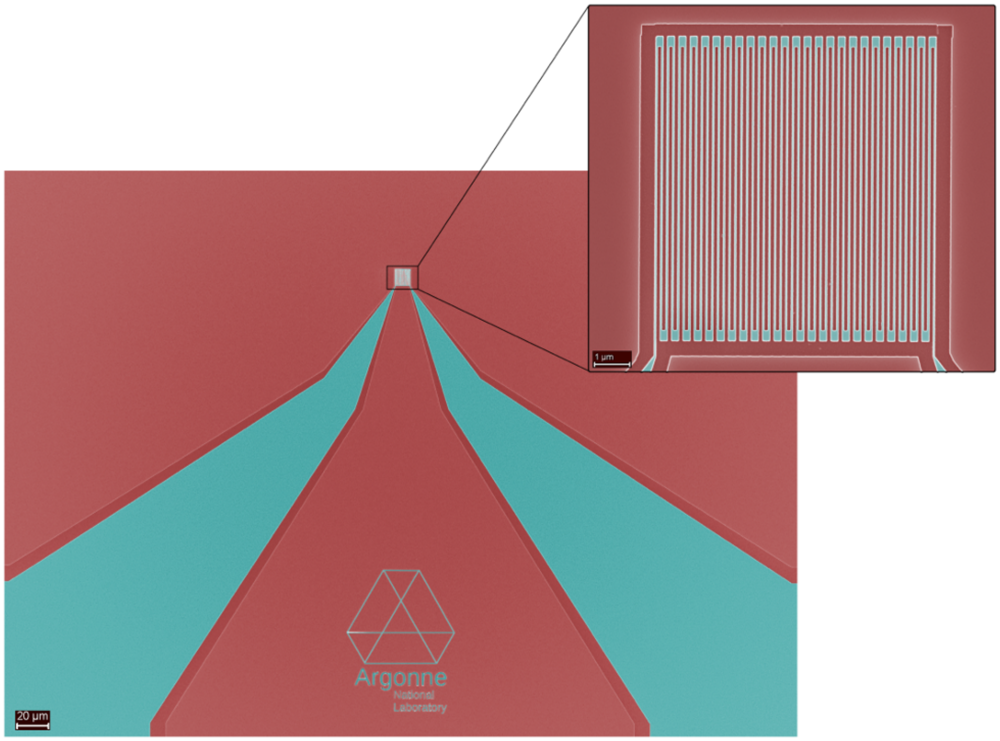

Figure 2: False color SEM micrograph showing a typical Superconducting nanowire device developed at Argonne. The inset shows a $10\,\mu\mathrm{m} \times 10\,\mu\mathrm{m}$ meandering nanowire geometry.

the noise threshold, can cause a change of more than 6 orders of magnitude in the wire resistance. This dramatic change can be detected without any significant signal preconditioning or amplification. SNSPDs were demonstrated to be superior in many figures of merit for the light detectors: timing resolution of less than 20 ps, a short reset time of approximately 10 ns, dark count rate of less than 10 counts/s/pixel, and a single photon resolution with more than 90% efficiency even at infra-red wavelengths [3].

The detection mechanism is based on change of quantum mechanical correlation between electrons (i.e. breaking of Cooper pairs only eliminates the entangled two-electron state, not the electrons themselves), which means that it doesn't alter the material by structural changes or changes to the single-electron system. This leads to longer detector lifetimes when compared to ionizing detectors, such as photomultiplier tubes and SiPMs, where redistribution of electronic densities during detection process generates strong electric fields and can cause irreversible microstructural defects.

Time Resolution Timing resolution is determined by the timing jitter of the device, which is the statistical variation of this time delay (typically reported as FWHM of the distribution). The

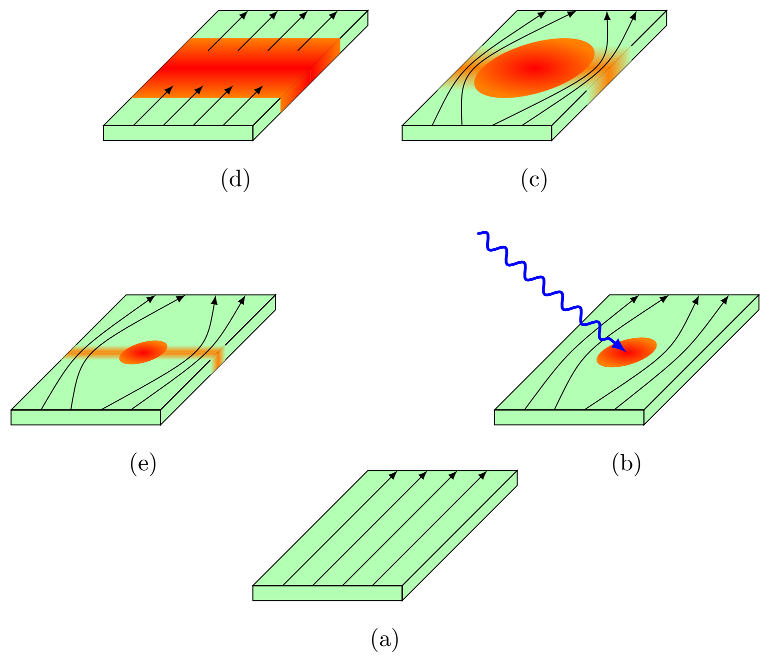

Figure 3: Schematic of the detection process through the hot spot formation after a photon absorption. Equilibrium superconductor is in green, orange to red depicts regions with increasingly suppressed order parameter and black lines depict the superconducting current density. Blue arrow is a schematic depiction of an incoming single photon.

variation has two contributions: an extrinsic variation due to geometry of the wire, where there's a different time delay depending on where along the length of the wire does the photon get absorbed (in a typical meander geometry, the wire length can reach a few mm) and jitter associated with the timing of the readout electronics [2]. Then there is the intrinsic variation that's due to the probabilistic nature of the processes that lead to the detection event. Typical values of timing jitter of SNSPD detectors arearound 15 ps and are dominated by the noise jitter of the readout [23],which can reduced down to 7 ps, a value due to geometric jitter [24]. On a short nano-bridge geometry, the intrinsic timing jitter of 2.7 ps [25] is reported, which is thought as the current fundamental limit to timing of the SNSPD devices.

High magnetic fields, low temperatures Typical experimental conditions of any collider experiment involve strong magnetic and often times cryogenic temperatures in close proximity to superconducting beam line magnets. At cryogenic temperatures, charge carrier freeze-out depletes Si-based photomultipliers and causes serious performance degradation [26]. The presence of strong magnetic fields also leads to decrease of detection efficiency, especially when using photomultiplier tubes.

As SNSPDs are superconducting, operation in cryogenic environments doesn't cause any degradation in their performance, and until recently, the only open question was their performance in magnetic fields. Low-dimensional superconductors (such as superconducting nanowires) can persist in a Meissner state at fields higher than those for bulk superconductors. Our group has committed significant effort towards developing technologies for scalable production of superconducting films that can sustain high magnetic fields [27] and we have recently demonstrated that superconducting nanowire detectors capable of high-rate, zero dark count detection in fields as high as 5 T [28], as shown in Figure 4, where the device operates with effectively zero dark count rate until the bias current is close to the field dependent I_c. While these field values should be sufficient for purposes of detectors in the EIC, we believe that higher field operation can be achieved by geometrical optimization [29].

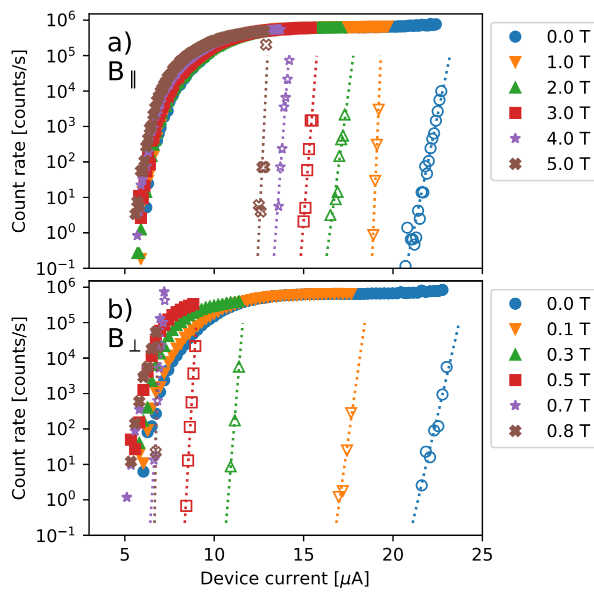

Figure 4: SNSPD bias current sweeps demonstrating performance at high fields [28]. Full symbols indicate total count rate and empty symbols are dark counts. Notice that it is possible to find an operating point with zero dark counts and fully saturated detection efficiency.

Radiation Hardness The performance in strong radiation field is an open question, we do however believe that superconductors can be more robust against radiation damage, as long as complex oxides (such as high-T_C superconducting cuprates) are avoided. This is especially true in the case of Niobium Nitride used for our devices because Nb has comparatively low neutron capture [30] and scattering [30,31] cross-sections and the short electron screening length of the material [32,33] makes it more robust against lattice defects. Preliminary results on our samples, exposed to the neutron flux near the beam dump of isotope separator (RAISOR) at the ATLAS facility at Argonne, indicate no degradation of superconducting properties. So far, the ongoing multiple month-long test still shows no noticeable difference, as can be seen in Figure 5. Compared to silicon detectors, where neutron capture causes nuclear decay and doping of semiconductor devices leading to their eventual failure, SNSPDs are anticipated to significantly more radiation hard.

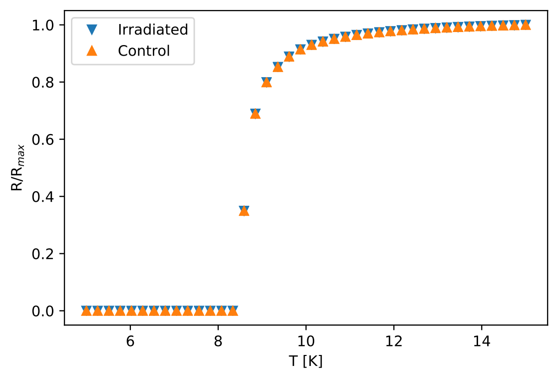

Figure 5: Comparison of the resistive superconducting transitions between a sample exposed to radiation environment of ATLAS accelerator and a clean control sample. It can be seen that the critical temperature of the sample remains unaffected by the neutron exposure.

3.2 Superconducting Nanowire Particle Detectors

Detection of energetic charged particles can be facilitated by two mechanisms. The first mechanism is scattering on the superconducting electrons directly, or indirectly through lattice phonons. The effect is no different from the photon absorption process – if the scattered particle deposits enough energy to break apart a Cooper pair, the excited quasi-particles will behave the same as those excited by photons.

The second mechanism is a thermal process [34]. In this thermal process, the hotspot in the nanowire is not created by diffusion and multiplication of quasi-particles, but by direct heat exchange with the microplasma in the particle track, creating a "hard" hotspot and completely circumventing the need for the first two steps sketched in Figure 3.

Ion detection The concept of detecting low energy molecules has already found a limited use in high-performance time-of-flight mass spectrometry [35], particularly in the form micron-sized of superconducting stripline detectors [36–39], which demonstrate that parallel superconducting wires provide both, high mass resolution and limited charge state state discrimination of ions [40]

In context of this proposal it is important to determine if SNSPDs are capable of detection of not particles in the few keV energy range, but particles with energies as high as 270 GeV. Detection of relativistic particles with SNSPDs has not been studied in literature, but the lower end of the range was explored previously [41], where high detection efficiencies of MeV α and β^- particles were reported. Over the timespan of 4 days, no degradation in noise, timing or efficiency have been observed, demonstrating good radiation hardness of SNSPDs in this (low) radiation environment.

Neutron detection Detection of charged particles is relatively straightforward because of comparatively high scattering cross sections with the lattice and electrons of the superconductor and substrate. There might be, however, desire to use SNSPDs to detect neutral particles such as neutrons. Working detection schemes utilizing SNSPDs are not yet developed but, for detection of neutrons, there exists a related technology that was used to demonstrate this capability: current biased kinetic inductance detectors (CBKID) [42–44] with a ^{10}B conversion layer.

In these devices a separate layer of ^{10}B is used [43,44], or a more direct approach can be used when detectors were fabricated out of superconducting MgB_2 [45]. ^{10}B in the devices converts neutrons into energetic ^{4}He and ^{7}Li ions that are detected using a differential readout of the CBKID delay line, which allows for a spatially-resolved measurement of neutron flux. Because the main neutron detection mechanism is through the conversion into charged particles, one can, in principle, substitute the CBKID devices with SNSPDs and construct a high-rate and high-speed detector of neutron flux with the same characteristics as discussed in the previous section.

To summarize, the superconducting nanowire detectors have multiple characteristics which make the unique in their field of photodetection, that can transfer into the field of particle detection:

- Ultrafast timing, which has been demonstrated to be on the $\lesssim 20$ ps scale, with a current record of 3 ps.
- Small basic pixel size, allowing for $\mu\mathrm{m}$ position precision if needed.
- Edgeless sensor configuration, where the sensitive element can be positioned to within a few 100 nm of the substrate edge, eliminating dead material in between the particle beam and the detector.
- Wide choice of substrates, where the detectors can be fabricated also on membranes as thin as few 10 μm, further cutting down on material thickness.
- Radiation hardness, which allows for longer service cycle of detectors operating in close proximity of the beam and interaction regions.

3.3 State-of-the-art Instrumentation Opportunities at the EIC

Concept 1: Novel forward detectors Far forward detection is achieved with Roman pot detectors which are movable and share a vacuum with the beam pipe. Figure 6 shows the current state of detection in the forward hadron region ending at ~ 35 m from the IR point. Instrumenting farther downstream would extend the detector acceptance in a critical region, enabling physics requiring extreme forward detection. In addition to leveraging the downstream magnets as extreme forward spectrometers, placing detection after the crab cavity removes the extra transverse smearing introduced by the crab cavity upstream of the IP.

Concept 2: Superconducting nanowire detector and superconducting magnet integration With many superconducting magnets at the EIC, there will be plenty of cooling power available, and with the tight space constraints, therefore integrating the very forward detectors with the magnets would mitigate space constraints of two separate cryogenic systems. In this case, the design of the magnets would need locations for these detectors to couple to the cooling system. This novel design would leverage the unique capabilities of the sensors to operate in strong magnetic fields at cryogenic temperatures to provide precision tracking and timing while sustaining operation in a high radiation environment. Studies with detailed beam line simulations (see Figure 7) are currently in progress.

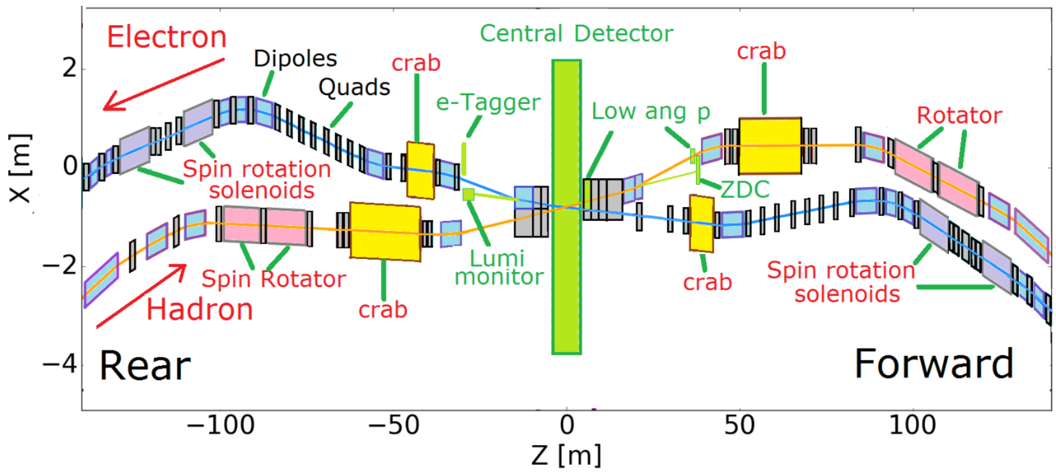

Figure 6: EIC IR with extended beam line magnets reproduced from the eRHIC design study [46].

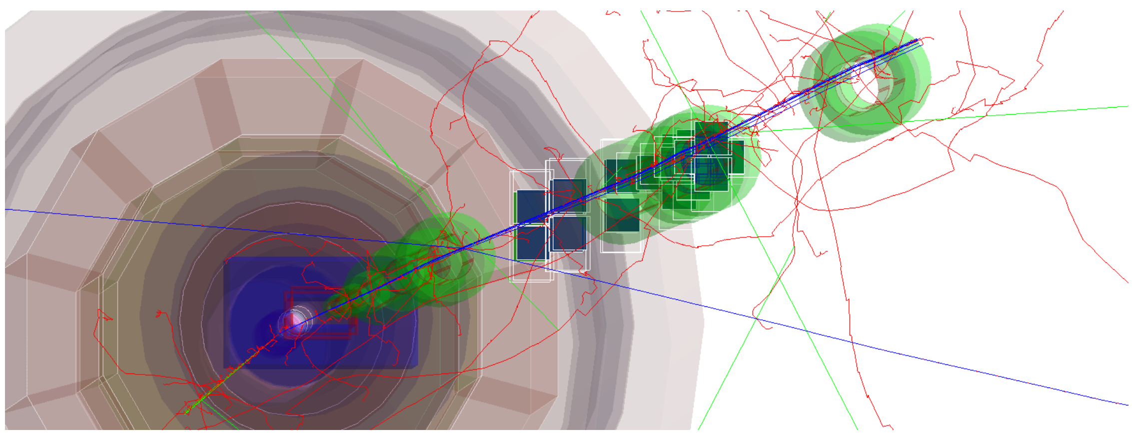

Figure 7: Simulation visualization of the forward hadron beam line extend up to the last quad before the spin rotator, located roughly 100 m downstream of the IP.

Concept 3: Neutral particle detector at zero degrees The forward hadron spectrometer has a large aperture to allow neutral particles to pass through to a zero-degree calorimeter (ZDC) shown in Figure 6. The ZDC will detect photons and neutrons with more demanding tracking requirements than previous detectors [47]. The small size, high radiation environment, close proximity to superconducting magnets, and particle tracking needs make it an attractive application for superconducting nanowire detectors. Instrumenting the front portion of the ZDC with a few cm^2 of tracking may dramatically improve performance with little modification to current designs.

4 Proposed Plan of Work

4.1 Device Fabrication

The pixels will initially have the standard meander geometry, with a wire thickness of roughly 15 nm, wire width of 100 nm, spacing between the wires of 100 nm (numbers can be relaxed, depending on future results). Basic pixel element will be $10 \times 10\ \mu\mathrm{m}^2$ (as shown in inset of Figure 2). Larger-scale devices will be prepared by parallel connection of these units into larger single-channel super-pixels.

The NbN thin films will be prepared by ion beam assisted sputtering as described in Refs. [27, 28]. This process allows for a high quality thin film synthesis on 6" wafers and at room temperature. Initial devices will be fabricated on bulk Si or SiN substrates and performance of devices on suspended $\mathrm{Si_3N_4}$ will be evaluated. Microfabrication process for superconducting devices suspended on thin membranes has already been developed for ground-based CMB studies with TES detectors. The devices will have critical temperatures $\gtrsim 9$ K, making them compatible with the cooling capabilities of the accelerator and will be able to perform in fields up to at least 5 T.

4.2 Device Characterization

After fabrication and dark testing, the devices will undergo standard characterization procedures with visible photons as described in our previous work [27, 28], including full characterisation of electronic and magnetic properties of the parent material and transport properties of the finished device. After we confirm nominal operation with photons, particle detection performance will be tested in-situ with radioactive particle source, to determine detection characteristics for charged particles up to ∼5 MeV, in magnetic fields.

4.3 Test Beam Characterization

We will conduct a first-of-its-kind test at the Fermilab Test Beam Facility [48] using 120 GeV protons, with the aid of an optical cryostat shown in Figure 8 (a closed system with a cooling power of $0.5\,\mathrm{W}$ at $4\,\mathrm{K}$). We will design a special thermal coupling and mount for the beam tests to minimize the amount of material supporting the wafer. Also, new windows for the vacuum chamber will be design to minimize the material upstream and down stream of the device. Finally an integrated LED pulsing system will be installed in the Vacuum chamber and used to monitor the device and study the rated dependence of particle detection.

4.4 Milestones

1. Fabricate 4×4 pixel array covering roughly $1\,\mathrm{mm}^2$ on a thin substrate.

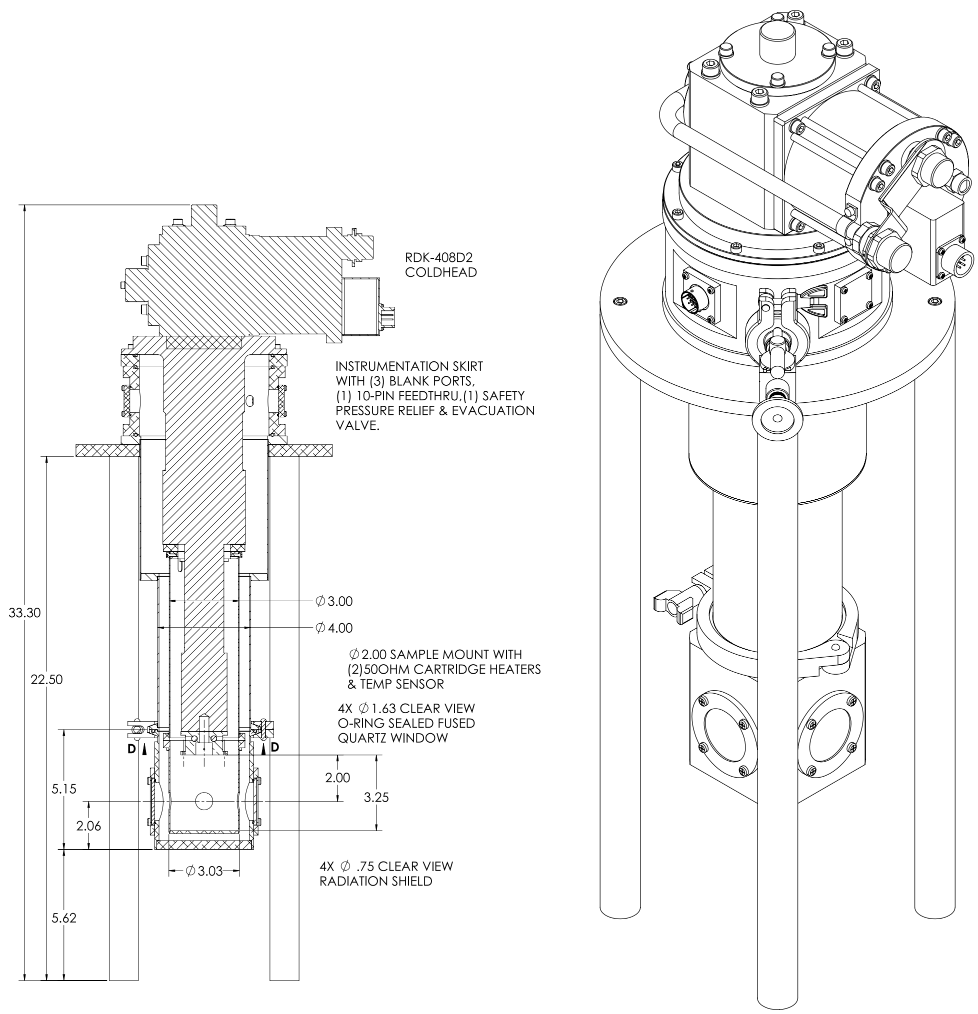

Figure 8: Diagram of the Janis SHI-4 cryostat to be used for device characterization and in-beam testing. The left shows the dimensions in inches. Not shown is the compressor.

2. Characterization of detector with a pulsed light source and radioactive sources in strong fields.

3. Design vacuum chamber windows and cold finger coupling mount for test beam measurements.

4. Full instrument readout of pixel array in optical cryostat.

5. Conduct in-beam pixel array test at the Fermilab Test Beam Facility using high energy protons.

item	Scenario 1	Scenario 2	Scenario 3
Test beam engineering Support	10k	10k	10k
Nanowire bias/readout electronics	25k	17k	9k
M&S	5k	5k	5k
total	40k	32k	24k

Table 1: Research Budget

4.5 Deliverables

1. Development of functioning 4×4 array of charged particle detectors covering an area of roughly 1 mm^2 .
2. Characterization of array performance with pulsed light source and low energy particles from radioactive sources.
3. Full device characterization with high energy proton beam.

5 Research Budget

Development of nanowire particle detectors is currently funded in part at ANL. The budget requested here reflects only the support needed to develop this cutting-edge technology for the EIC.

Scenario 1 A budget of $40k is requested to support the planned R&D. An allocation of $10k is for engineer support to design the cold finger, vacuum entrance windows, and other mechanical support for operation in the test beam. The $25k request for nanowire bias and readout electronics will allow for 8 channels of high speed readout. The nanowire electronics are commercially available from Quantum Opus [49]. The remaining $5k will go to M&S for items such as cables, connectors, and vacuum feed-throughs.

Scenario 2 Under a 20% reduction in the requested budget, we would purchase only 5 channels of readout. This would mean only having four channels of simultaneous high speed readout.

Scenario 3 Like the previous scenario, under a 40% reduction in the requested budget, we would purchase fewer channels of readout (3 channels in this case).

References

[1] GN Gol'Tsman, O Okunev, G Chulkova, A Lipatov, A Semenov, K Smirnov, B Voronov, A Dzardanov, C Williams, and Roman Sobolewski. Picosecond superconducting single-photon optical detector. *Applied physics letters*, 79(6):705–707, 2001.

[2] Junjie Wu, Lixing You, Sijing Chen, Hao Li, Yuhao He, Chaolin Lv, Zhen Wang, and Xiaoming Xie. Improving the timing jitter of a superconducting nanowire single-photon detection system. *Applied optics*, 56(8):2195–2200, 2017.

[3] F Marsili, Varun B Verma, Jeffrey A Stern, S Harrington, Adriana E Lita, Thomas Gerrits, Igor Vayshenker, Burm Baek, Matthew D Shaw, Richard P Mirin, et al. Detecting single infrared photons with 93% system efficiency. *Nature Photonics*, 7(3):210, 2013.

[4] WeiJun Zhang, LiXing You, Hao Li, Jia Huang, ChaoLin Lv, Lu Zhang, XiaoYu Liu, JunJie Wu, Zhen Wang, and XiaoMing Xie. Nbn superconducting nanowire single photon detector with efficiency over 90% at 1550 nm wavelength operational at compact cryocooler temperature. *Science China Physics, Mechanics & Astronomy*, 60(12):120314, 2017.

[5] Hiroyuki Shibata, Kaoru Shimizu, Hiroki Takesue, and Yasuhiro Tokura. Ultimate low system dark-count rate for superconducting nanowire single-photon detector. *Optics letters*, 40(14):3428–3431, 2015.

[6] Jiang Zhu, Yajun Chen, Labao Zhang, Xiaoqing Jia, Zhijun Feng, Ganhua Wu, Xiachao Yan, Jiquan Zhai, Yang Wu, Qi Chen, et al. Demonstration of measuring sea fog with an snspd-based lidar system. *Scientific reports*, 7(1):1–7, 2017.

[7] Hiroki Takesue, Shellee D Dyer, Martin J Stevens, Varun Verma, Richard P Mirin, and Sae Woo Nam. Quantum teleportation over 100 km of fiber using highly efficient superconducting nanowire single-photon detectors. *Optica*, 2(10):832–835, 2015.

[8] Hiroki Takesue, Sae Woo Nam, Qiang Zhang, Robert H Hadfield, Toshimori Honjo, Kiyoshi Tamaki, and Yoshihisa Yamamoto. Quantum key distribution over a 40-db channel loss using superconducting single-photon detectors. *Nature photonics*, 1(6):343, 2007.

[9] Jun Chen, Joseph B Altepeter, Milja Medic, Kim Fook Lee, Burc Gokden, Robert H Hadfield, Sae Woo Nam, and Prem Kumar. Demonstration of a quantum controlled-not gate in the telecommunications band. *Physical review letters*, 100(13):133603, 2008.

[10] Chandra M Natarajan, Michael G Tanner, and Robert H Hadfield. Superconducting nanowire single-photon detectors: physics and applications. *Superconductor science and technology*, 25(6):063001, 2012.

[11] A. Accardi et al. Electron Ion Collider: The Next QCD Frontier: Understanding the glue that binds us all. *Eur. Phys. J. A*, 52(9):268, 2016.

[12] 1st eic yellow report workshop at temple university, 2020.

[13] 2nd eic yellow report workshop at pavia university, 2020.

[14] A. Dumitru, O. Evdokimov, A. Metz, C. Muñoz Camacho. YR Physics WG Conveners: overview and progress report. In *2nd EIC Yellow Report Workshop at Pavia University*, May 2020.

[15] Engineering "National Academies of Sciences and Medicine". *An Assessment of U.S.-Based Electron-Ion Collider Science*. The National Academies Press, Washington, DC, 2018.

[16] E.C. Aschenauer, A.Tricoli, et al. A proposal for silicon detectors with high position and timing resolution as roman pots at eic, May 2019.

[17] A. V. Belitsky and A. V. Radyushkin. Unraveling hadron structure with generalized parton distributions. *Phys. Rept.*, 418:1–387, 2005.

[18] M. Hattawy et al. First Exclusive Measurement of Deeply Virtual Compton Scattering off ^{4}He: Toward the 3D Tomography of Nuclei. *Phys. Rev. Lett.*, 119(20):202004, 2017.

[19] Whitney Armstrong et al. Partonic Structure of Light Nuclei. *JLab PAC*, 2017.

[20] AN Zotova and D Yu Vodolazov. Photon detection by current-carrying superconducting film: A time-dependent ginzburg-landau approach. *Physical Review B*, 85(2):024509, 2012.

[21] AD Semenov, RS Nebosis, Yu P Gousev, MA Heusinger, and KF Renk. Analysis of the nonequilibrium photoresponse of superconducting films to pulsed radiation by use of a two-temperature model. *Physical Review B*, 52(1):581, 1995.

[22] Alex D Semenov, Gregory N Gol'tsman, and Alexander A Korneev. Quantum detection by current carrying superconducting film. *Physica C: Superconductivity*, 351(4):349–356, 2001.

[23] Q Zhao, L Zhang, T Jia, L Kang, W Xu, J Chen, and P Wu. Intrinsic timing jitter of superconducting nanowire single-photon detectors. *Applied Physics B*, 104(3):673–678, 2011.

[24] Niccolò Calandri, Qing-Yuan Zhao, Di Zhu, Andrew Dane, and Karl K Berggren. Superconducting nanowire detector jitter limited by detector geometry. *Applied Physics Letters*, 109(15):152601, 2016.

[25] BA Korzh, Qing-Yuan Zhao, S Frasca, JP Allmaras, TM Autry, Eric A Bersin, M Colangelo, GM Crouch, AE Dane, T Gerrits, et al. Demonstrating sub-3 ps temporal resolution in a superconducting nanowire single-photon detector. *arXiv preprint arXiv:1804.06839*, 2018.

[26] M Biroth, P Achenbach, E Downie, and A Thomas. Silicon photomultiplier properties at cryogenic temperatures. *Nuclear Instruments and Methods in Physics Research Section A: Accelerators, Spectrometers, Detectors and Associated Equipment*, 787:68–71, 2015.

[27] Tomas Polakovic, Sergi Lendinez, John E. Pearson, Axel Hoffmann, Volodymyr Yefremenko, Clarence L. Chang, Whitney Armstrong, Kawtar Hafidi, Goran Karapetrov, and Valentine Novosad. Room temperature deposition of superconducting niobium nitride films by ion beam assisted sputtering. *APL Materials*, 6(7):076107, 2018.

[28] T. Polakovic, W.R. Armstrong, V. Yefremenko, J.E. Pearson, K. Hafidi, G. Karapetrov, Z.-E. Meziani, and V. Novosad. Superconducting nanowires as high-rate photon detectors in strong magnetic fields. *Nucl. Instrum. Meth. A*, 959:163543, 2020.

[29] Ilya Charaev, Alexey Semenov, Stefan Doerner, G Gomard, Konstantin Ilin, and Michael Siegel. Current dependence of the hot-spot response spectrum of superconducting single-photon detectors with different layouts. *Superconductor Science and Technology*, 30(2):025016, 2016.

[30] G Reffo, F Fabbri, K Wisshak, and F Käppeler. Fast neutron capture cross sections and related gamma-ray spectra of niobium-93, rhodium-103, and tantalum-181. *Nuclear Science and Engineering*, 80(4):630–647, 1982.

[31] AB Smith, PT Guenther, and JF Whalen. Neutron total and scattering cross sections of niobium in the continuum region. *Zeitschrift für Physik*, 264(5):379–398, 1973.

[32] SP Chockalingam, Madhavi Chand, Anand Kamlapure, John Jesudasan, Archana Mishra, Vikram Tripathi, and Pratap Raychaudhuri. Tunneling studies in a homogeneously disordered s-wave superconductor: Nbn. *Physical Review B*, 79(9):094509, 2009.

[33] E Piatti, A Sola, D Daghero, GA Ummarino, F Laviano, JR Nair, C Gerbaldi, R Cristiano, A Casaburi, and RS Gonnelli. Superconducting transition temperature modulation in nbn via edl gating. *Journal of Superconductivity and Novel Magnetism*, 29(3):587–591, 2016.

[34] NK Sherman. Superconducting nuclear particle detector. *Physical Review Letters*, 8(11):438, 1962.

[35] Nobuyuki Zen, Yigang Chen, Koji Suzuki, Masataka Ohkubo, Shigehito Miki, and Zhen Wang. Development of superconducting strip line detectors (sslds) for time-of-flight mass spectrometers (tof-ms). *IEEE transactions on applied superconductivity*, 19(3):354–357, 2009.

[36] A Casaburi, E Esposito, M Ejrnaes, K Suzuki, M Ohkubo, S Pagano, and R Cristiano. A 2×2 mm2 superconducting strip-line detector for high-performance time-of-flight mass spectrometry. *Superconductor Science and Technology*, 25(11):115004, 2012.

[37] M Ohkubo. Superconducting detectors for particles from atoms to proteins. *Physica C: Superconductivity*, 468(15-20):1987–1991, 2008.

[38] K Suzuki, S Miki, S Shiki, Y Kobayashi, K Chiba, Z Wang, and M Ohkubo. Ultrafast ion detection by superconducting nbn thin-film nanowire detectors for time-of-flight mass spectrometry. *Physica C: Superconductivity*, 468(15-20):2001–2003, 2008.

[39] Kyosuke Sano, Yoshihiro Takahashi, Yuki Yamanashi, Nobuyuki Yoshikawa, Nobuyuki Zen, and Masataka Ohkubo. Demonstration of single-flux-quantum readout circuits for time-of-flight mass spectrometry systems using superconducting strip ion detectors. *Superconductor Science and Technology*, 28(7):074003, 2015.

[40] Koji Suzuki, Shigetomo Shiki, Masahiro Ukibe, Masaki Koike, Shigehito Miki, Zhen Wang, and Masataka Ohkubo. Hot-spot detection model in superconducting nano-stripline detector for kev ions. *Applied physics express*, 4(8):083101, 2011.

[41] Hatim Azzouz, Sander N Dorenbos, Daniel De Vries, Esteban Bermúdez Ureña, and Valery Zwiller. Efficient single particle detection with a superconducting nanowire. *AIP Advances*, 2(3):032124, 2012.

[42] Alex Malins, Masahiko Machida, The Dang Vu, Kazuya Aizawa, and Takekazu Ishida. Monte carlo radiation transport modelling of the current-biased kinetic inductance detector. *Nuclear Instruments and Methods in Physics Research Section A: Accelerators, Spectrometers, Detectors and Associated Equipment*, 953:163130, 2020.

[43] Yuki Iizawa, Hiroaki Shishido, Kazuma Nishimura, Kenji M Kojima, Tomio Koyama, Kenichi Oikawa, Masahide Harada, Shigeyuki Miyajima, Mutsuo Hidaka, Takayuki Oku, et al. Energy-resolved neutron imaging with high spatial resolution using a superconducting delay-line kinetic inductance detector. *Superconductor Science and Technology*, 32(12):125009, 2019.

[44] Hiroaki Shishido, Yuya Miki, Hiroyuki Yamaguchi, Yuki Iizawa, Kenji M Kojima, Tomio Koyama, Kenichi Oikawa, Masahide Harada, Shigeyuki Miyajima, Mutsuo Hidaka, et al. High-speed neutron imaging using a current-biased delay-line detector of kinetic inductance. *Physical Review Applied*, 10(4):044044, 2018.

[45] Naohito Yoshioka, Ikutaro Yagi, Hiroaki Shishido, Tsutomu Yotsuya, Shigeyuki Miyajima, Akira Fujimaki, Shigehito Miki, Zhen Wang, and Takekazu Ishida. Current-biased kinetic inductance detector using mgb_2 nanowires for detecting neutrons. *IEEE transactions on applied superconductivity*, 23(3):2400604–2400604, 2013.

[46] A. Arno et al. Eic deisgn study, 2019.

[47] Yuji Goto et al. Development of position sensitive zero degree calorimeter for eic, January 2020.

[48] Fermilab test beam facility, https://ftbf.fnal.gov/.

[49] Quantumopus nanowire electronics, https://www.quantumopus.com/web/wp-content/uploads/2017/01/NANOWIRE-ELECTRONICS-DATASHEET-20170125.pdf.